

Magnetism and Structure of Epitaxial Face-Centered Tetragonal Fe Thin Films

B. ROLDAN CUENYA, M. DOI*, T. RUCKERT, W. KEUNE and T. STEFFL¹

Laboratorium für Angewandte Physik, Gerhard-Mercator-Universität Duisburg, D-47048 Duisburg, Germany

¹*Laboratorium für Tieftemperaturphysik, Gerhard-Mercator-Universität Duisburg, D-47048 Duisburg, Germany*

(Received February 1, 2000)

The structural and magnetic properties of Fe films grown by molecular beam epitaxy on Cu₃Au(001) and on Pd(001), and of Fe films in a [Fe(15Å)/Pd(40Å)]₃₀ multilayer, have been determined by electron diffraction (RHEED, LEED), X-ray diffraction, ⁵⁷Fe Mössbauer spectroscopy (CEMS), or SQUID magnetometry. Very thin Fe films are found to have a tetragonally compressed fcc (fct) structure and an enhanced saturation hyperfine field relative to that of bulk bcc Fe. The Fe magnetization in the Fe/Pd multilayer is remarkably enhanced with respect to that of bulk bcc Fe. Our results demonstrate that thin fct Fe films in these systems are in a ferromagnetic high-moment state with an Fe atomic volume (or Wigner-Seitz radius) which is rather close to that of bulk bcc Fe due to lattice relaxation.

§1. Introduction

Face-centered cubic (fcc or γ -) iron has been a fascinating system until today because of its intriguing magnetic properties and its delicate interplay between magnetism and structure.^{1–3)} Interest for this system is stimulated by the extreme atomic-volume dependence of the ground-state magnetic properties (magnetovolume instabilities) predicted theoretically for bulk fcc Fe,^{1–3)} and observed experimentally for epitaxial fcc-like Fe thin films (for a brief review, see, for instance, Ref. 4). The prediction that both the magnetic exchange coupling and the Fe magnetic moment in fcc Fe depend strongly on interatomic distances initiated a vast number of investigations on epitaxial fcc or fcc-like Fe thin films on Cu(001) and other related substrates.^{4–6)} Such epitaxial growth allows the low-temperature stabilization of the high-temperature fcc Fe phase in form of a metastable thin film. The basis for epitaxial growth of fcc Fe films on fcc Cu(001) is the similarity of lattice parameters of Cu ($a = 3.615$ Å at 295 K) and γ -Fe (3.588 Å at 293 K, extrapolated from equilibrium (bulk) γ -Fe data above 910 °C,⁷⁾ or 3.5757 Å at 80 K, measured on coherent γ -Fe precipitates in a Cu matrix⁸⁾). It is generally accepted now that room-temperature (RT) grown fcc-type Fe films on Cu(001) in the 2–4 monolayer (ML) thickness range are ferromagnetic (FM) with a high Fe-spin magnetic moment (high spin state) of $2.8 \mu_B$ ⁹⁾ and a large saturation hyperfine (hf) field of ~ 31 – 34 T⁵⁾ (accidentally similar to that of bcc Fe), and has the fct structure with an expanded atomic volume, including some 'buckling' of Fe atoms.¹⁰⁾ For thicker (RT-grown) Fe films on Cu(001) in the ~ 5 – 10 ML range the ideally fcc interior with a smaller atomic volume is paramagnetic at RT and very likely antiferromagnetic (AFM) at low T with a low hf field, B_{hf} , of ~ 1 – 2 T,⁵⁾ while FM is re-

stricted to the film-vacuum surface region^{5,11,12)} with an average Fe spin moment of $0.8 \mu_B$.⁹⁾ Until recently it was assumed that the epitaxial growth of fcc-type Fe on Cu(001) is pseudomorphous,¹³⁾ which would result in a strained fcc-Fe lattice due to the misfit of ~ 0.7 % with respect to the Cu lattice. However, a recent Reflection High Energy Electron Diffraction (RHEED) study proves that epitaxial fcc-type Fe films on Cu(001) are non-pseudomorphous and grow strain free.¹⁴⁾

The magnetic hf field, B_{hf} , measured, at low T (near saturation) is roughly proportional to the local Fe atomic moment. Therefore, a measurement of B_{hf} provides information about possible high or low Fe magnetic moments in Fe films. Fig. 1 exhibits a plot of the saturation hf field versus the Wigner-Seitz radius r_{ws} ¹⁵⁾ (in atomic units) for different fcc-like Fe systems.⁴⁾ (Note that $r_{ws} = 2.67$ a.u. for Cu at 300 K). B_{hf} was measured by ⁵⁷Fe Mössbauer spectroscopy. Fig. 1 demonstrates unambiguously that there is a transition from a low-moment fcc-Fe state to a high-moment fcc-like Fe state. The transition seems to occur around $r_{ws} \sim 2.69$ a.u., which is in good agreement with theoretical predictions for bulk fcc Fe.^{1–3)}

A word of caution is justified in view of the r_{ws} values associated with the data points in Fig. 1. The only experimentally determined r_{ws} values are those of 5–10 ML thick low-moment fcc-Fe/Cu(001) ($r_{ws} = 2.653$ a.u., full square) and 2–4 ML thick high-moment fct-Fe/Cu(001) ($r_{ws} = 2.705$ a.u., full circle), reported^{10,13,16)} on the basis of quantitative LEED results, as well as the value of $r_{ws} = 2.643$ a.u. (open triangle) reported for AFM low-moment γ -Fe precipitates in a Cu matrix.⁸⁾ The other r_{ws} data in Fig. 1 are nominal values that were obtained under the following assumptions: (i) the lattice parameter of AFM low-moment fcc-Fe precipitates in a Cu_{1–x}Al_x matrix (open triangles) is expanded with increasing x in proportion to the lattice parameter increase of the matrix^{17,18)}; (ii) the FM high-moment fct-Fe films in Fe/Cu_{1–x}Au_x(001) multilayers (open circles¹⁹⁾) and

* permanent address: Department of Materials Science and Engineering, Nagoya University, Nagoya 464-01, Japan

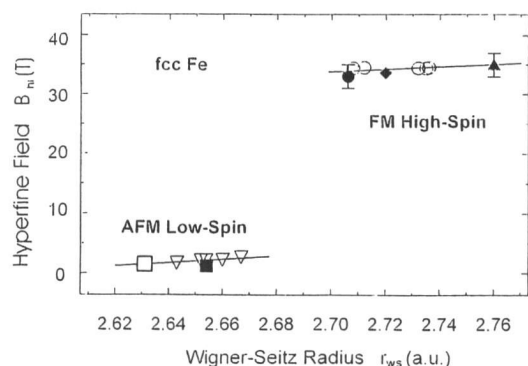


Fig. 1. Hyperfine field near magnetic saturation as a function of the Wigner-Seitz radius, r_{ws} . Full square: 300-K grown 5-10 ML fcc-Fe/Cu(001) at 35 K. Full circle: 300-K grown and 100-K grown fct-Fe/Cu(001) and 100-K grown 7 ML fct-Fe/Cu(001) at 40-55 K. Full triangle: 300-K grown 5 ML fcc-Fe/Cu₃Au(001) at 30 K. Open circles: 275-K grown [fcc-Fe/Cu_{100-x}Au_x(001)] multilayers at 15 K. Open triangles: fcc Fe precipitates in Cu_{100-x}Al_x matrix at 4.2 K. Open square: fcc Fe precipitates in Cu₈₆Al₁₄ matrix under high pressure (58 kbar) at 4.2 K. Full diamond: 475-K grown [hcp-Fe/Ru(0001)] multilayer at 4.2 K. (atomic volume = $4\pi r_{ws}^3/3$; 1 a.u. = 0.529 CII) (figure taken from ref. 4)

on ordered Cu₃Au(001) (full triangle¹⁸) expand their atomic volume proportional to that of the substrate. As compared to Cu, atomically ordered Cu₃Au has an expanded lattice parameter of 3.75 Å.

In the present work we concentrate on the question whether assumption (ii) is justified. For this purpose a MBE-grown 4.0 ML thick fct-Fe film on an atomically ordered Cu₃Au(001) substrate was investigated by RHEED, LEED and ⁵⁷Fe conversion electron Mössbauer spectroscopy (CEMS). RHEED allows the precise determination of the in-plane lattice parameter of the growing Fe film relative to that of the Cu₃Au(001) substrate, while the intensity-voltage (I/V-) dependence of the specular (00) beam in LEED (Low Energy Electron Diffraction) permits a good estimate of the out-of-plane lattice parameter. Both parameters combined then provide the Fe atomic volume in the film. Moreover, we report upon the hf field in [Fe/Pd]_n multilayers, for which stabilization of high-moment fcc Fe has been reported recently.²⁰ In this case Fe is embedded in Pd which has a very large lattice parameter of 3.89 Å ($r_{ws} = 2.868$ a.u.) as compared to that of Cu.

§2. Experimental

The Fe(4ML)/Cu₃Au(001) sample was prepared by molecular beam epitaxy (MBE) in an ultrahigh vacuum (UHV) system with a base pressure of 6×10^{-11} mbar. In order to obtain a clean Cu₃Au(001) surface the single crystal surface was mechanically polished first, followed by Ar⁺ sputter cleaning in the UHV system (1 kV, 5×10^{-5} mbar Ar pressure) at 200 °C for 2-3 h, until no impurities could be detected by Auger electron spectroscopy (AES). Subsequent Ar⁺ sputter smoothing of the surface (0.5 kV, and 5.5×10^{-5} mbar Ar pressure) was achieved at 200 °C for 40 min. The atomically

ordered Cu₃Au(001) surface was obtained after subsequent sequential annealing at 447 °C for 1 h, at 417 °C for 1 h, and at 327 °C for 15 h. Several cycles of sputter smoothing and annealing were performed until sharp (-1/2, 1/2) and (1/2, -1/2) superstructure streaks of the ordered (2×2) Cu₃Au(001) surface were obtained in the RHEED pattern, in addition to the fundamental (-1,1) and (1,-1) streaks (Fig. 2(a)). Natural Fe films (purity: 99.9985 at.%) or ⁵⁷Fe films (isotopic enrichment: 95.5 %) were grown at a substrate temperature of 40 °C and at a deposition rate of ~ 1.8 Å/min, with a deposition pressure of $\sim 1.5 \times 10^{-10}$ mbar. The deposition rate and film thickness of 4.0 ± 0.4 ML was measured by a quartz microbalance previously calibrated by RHEED intensity oscillations during growth of fcc Fe films on Cu(001). RHEED patterns were recorded during growth by a CCD camera connected to a computer for data storage and later analysis. I/V-curves of the specular (0,0) LEED spot were measured by the same CCD camera/computer data storage system.

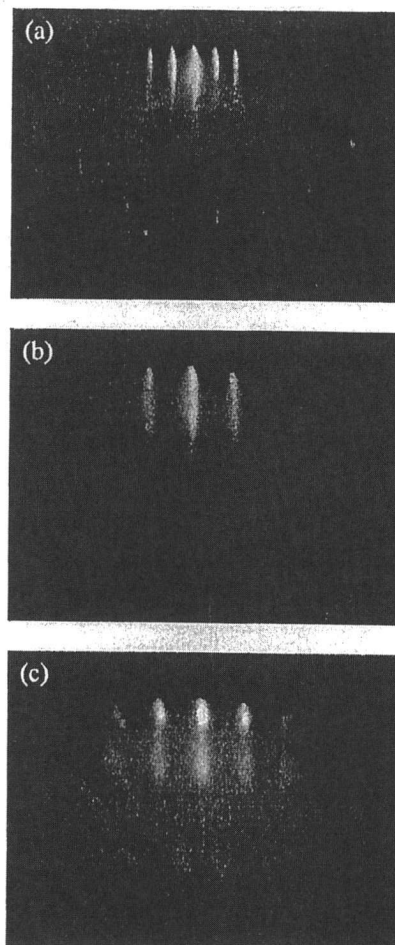


Fig. 2. RHEED patterns of the clean atomically ordered Cu₃Au(001) surface (a); Cu₃Au(001) covered with 6 ML fcc-like Fe (b); Cu₃Au(001) covered with 6 ML bcc Fe (b); Cu₃Au(001) covered with 13 ML bcc Fe. ([100] azimuth, beam voltage 12 kV, beam current 40 μA).

The Fe/Pd multilayer was room-temperature grown by alternating UHV vapor deposition at about 1×10^{-9}

mbar on an $\text{Al}_2\text{O}_3(11\text{-}20)$ (sapphire) substrate which carried a Pd buffer layer. The sapphire substrate was cleaned in ethanol followed by annealing at 400°C in UHV. A 4 Å thick Fe seed layer (deposited at 395°C) was required²¹⁾ before the 300 Å thick Pd buffer layer was deposited (also at 395°C). After cooling to RT the $[\text{Fe}(15\text{Å})/\text{Pd}(40\text{Å})]\times 30$ multilayer was deposited with rates of 4.8 Å/min (Fe) and 9.0 Å/min (Pd), as measured by a calibrated quartz microbalance. 13% ^{57}Fe enrichment was used for Fe.

The high-angle X-ray diffraction diagram of the multilayer is shown in Fig. 3, together with that of the clean sapphire substrate. The observation of Pd(111) and Pd(222) Bragg reflections together with Pd(200) and Pd(400) reflections indicates that epitaxial growth is not ideal, but a texture of preferred (111)- and (200)-oriented grains appears. The observed satellite peaks around the (111), (200) and (222) reflections and their angular separation provide a proof of the high-quality multilayer structure with a period of 55 Å.

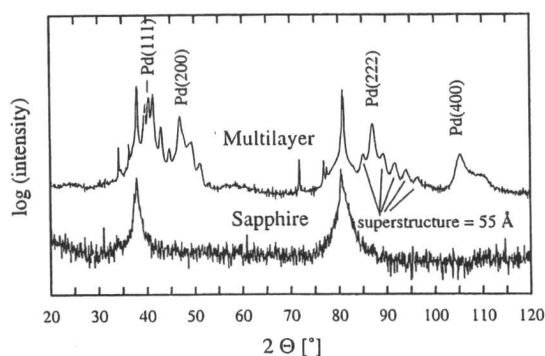


Fig. 3. High-angle X-ray diffraction diagram of the $[\text{Fe}(15\text{Å})/\text{Pd}(40\text{Å})]\times 30$ multilayer on 300 Å-Pd buffer/sapphire substrate (top), and of clean $\text{Al}_2\text{O}_3(11\text{-}20)$ sapphire substrate (bottom). ($\text{Cu-K}\alpha$ radiation).

^{57}Fe CEMS spectra were measured in-situ in UHV on the $\text{Fe}/\text{Cu}_3\text{Au}(001)$ sample and ex-situ on the Fe/Pd multilayer. Electrons emitted from the sample surface after the nuclear resonant absorption were detected by a channeltron. A ^{57}Co -in-Rh Mössbauer source was used. The incoming γ -ray direction was normal to the film plane.

§3. Results and Discussion

3.1 $\text{Fe}/\text{Cu}_3\text{Au}(001)$

Typical RHEED patterns of 6 ML $\text{Fe}/\text{Cu}_3\text{Au}(001)$ and 13 ML $\text{Fe}/\text{Cu}_3\text{Au}(001)$ are shown in Fig. 2(b) and (c), respectively. The half-integer (2×2) superstructure streaks of the ordered $\text{Cu}_3\text{Au}(001)$ surface disappear after a small Fe coverage, and only the fundamental streaks remain, as can be seen in Fig. 2(b). This demonstrates that a 6 ML Fe film grows epitaxially with a flat surface, and its in-plane lattice is approximately in registry with the $\text{Cu}_3\text{Au}(001)$ surface mesh, like the fcc structure requires. At 13 ML coverage the RHEED pattern changes to a dot-type pattern that is typically observed in 3-dimensional (3D) film growth; this pattern indicates

3D growth of epitaxial bcc Fe.

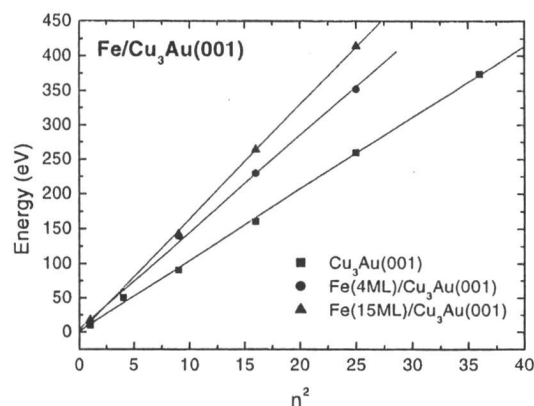


Fig. 4. Measured Bragg energy E_n of specular (0,0) LEED beam versus n^2 for the clean ordered $\text{Cu}_3\text{Au}(001)$ surface (full square), 4 ML $\text{Fe}/\text{Cu}_3\text{Au}(001)$ (circle), and 15 ML $\text{Fe}/\text{Cu}_3\text{Au}(001)$ (triangle). The straight lines are least-squares fits.

The separation of the RHEED streaks in reciprocal space is a measure for the in-plane lattice parameter in real space²²⁾ in a direction perpendicular to the scattering plane. The in-plane lattice spacing of the Fe film relative to that of the $\text{Cu}_3\text{Au}(001)$ substrate was determined from the measured distance in reciprocal space between the (-1,1) and (1,-1) streaks. By least-squares fitting the measured intensity profile of the RHEED streaks with a Lorentzian line the position of the RHEED reflections (and consequently the in-plane lattice parameter) can be obtained with high precision.¹⁴⁾ For the 4.0 ML Fe film on $\text{Cu}_3\text{Au}(001)$ we obtained an enhanced value of $2.685 \pm 0.006\text{ Å}$ for the atomic nearest neighbor distance within the (001) plane, as compared to $a/\sqrt{2} = 2.652\text{ Å}$ for that of Cu_3Au . For 13 ML Fe coverage we measured an in-plane atomic nearest neighbor distance of $2.819 \pm 0.013\text{ Å}$, which is closer to the lattice parameter of bcc Fe ($a = 2.866\text{ Å}$), indicating that a transition to distorted bcc Fe has occurred.

The lattice parameter c_0 in the direction perpendicular to the film plane can be determined from the electron energy dependence of the intensity of the specularly reflected (0,0) LEED beam. The Bragg energy E_n of the n -th intensity maximum at perpendicular incidence of the primary electron beam is given by

$$E_n = (2\pi n/c_0)2h^2/8\pi^2m + E_0$$

in the kinematic approximation.²³⁻²⁵⁾ E_0 is the inner potential, and n is an integer giving the order of the Bragg intensity maximum. Fig. 2 shows the result of the LEED measurement. The slope of the straight lines is a measure of the out-of-plane lattice parameter c_0 . Fig. 3 shows a plot of c_0 versus Fe coverage, obtained from Fig. 2. c_0 of the clean ordered $\text{Cu}_3\text{Au}(001)$ is in good agreement with the known bulk value of fcc Cu_3Au ($3.75\text{ C}\Pi$). c_0 decreases considerably to a value of $3.25 \pm 0.06\text{ Å}$ at 4 ML Fe coverage, while at the same time the in-plane atomic distance increases from 2.652 Å for Cu_3Au to 2.685

Å for 4 ML Fe, as obtained from RHEED. This demonstrates that for 4 ML Fe/Cu₃Au(001) the Fe lattice is a tetragonally compressed face-centered (fct) lattice with an Fe atomic volume V_{at} of $11.71 \pm 0.27 \text{ Å}^3$ or Wigner-Seitz radius r_{ws} of $2.664 \pm 0.019 \text{ a.u.}$ It is remarkable that this r_{ws} value agrees well within error bars with $r_{\text{ws}} = 2.667 \text{ a.u.}$ of bulk bcc Fe, although the film structure is fct and by no means bcc.

For 15 ML Fe on Cu₃Au(001) the LEED result provides an out-of-plane lattice parameter c_0 of $3.00 \pm 0.02 \text{ Å}$, whereas for the in-plane nearest-neighbor distance we take the same RHEED value (2.819 Å) as for 13 ML Fe on Cu₃Au. Thus, for 13-15 ML Fe coverage on Cu₃Au $V_{\text{at}} = 11.92 \pm 0.19 \text{ Å}^3$ or $r_{\text{ws}} = 2.679 \pm 0.014 \text{ a.u.}$ Also this value agrees within error bars with r_{ws} of bulk bcc Fe of 2.667 a.u. Since the in-plane as well as the out of plane lattice parameters are closer to that of bcc Fe we may consider the structure of 13-15 ML Fe/Cu₃Au(001) as distorted bcc (expanded bct structure).

The Mössbauer (CEM) spectrum of the 4 ML fct Fe film on Cu₃Au(001) at 25 K is shown in Fig. 5. The spectrum demonstrates that this film is magnetically ordered. The outer lines of the Zeeman sextet are very broad, indicating a distribution of hyperfine fields, $P(B_{\text{hf}})$. Further, the lines number 2 and 5 (i.e. the $\Delta m = 0$ Zeeman transitions) are nearly missing, indicating a spontaneous preferred Fe spin direction perpendicular to the film plane (perpendicular magnetic anisotropy, PMA). This is the first microscopic observation of PMA in Fe/Cu₃Au(001). Ferromagnetism and PMA have been observed earlier in Fe/Cu₃Au(001) by macroscopic measurement techniques.^{24,26-29} A preliminary least-squares fit of the experimental spectrum with a distribution of hf fields (Fig. 5) yields a most probable (peak) hf-field value of 36 T at 25 K, which is enhanced by $\sim 6 \%$ relative to B_{hf} of bulk bcc Fe at the same temperature. Therefore, the 4 ML thick fct-Fe film on Cu₃Au(001) is clearly in a high-moment Fe state.

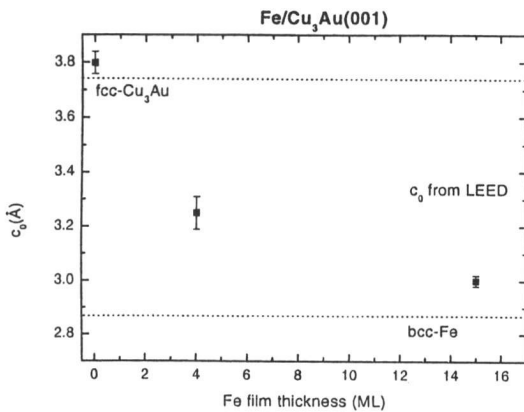


Fig. 5. Out-of-plane lattice parameter c_0 versus Fe coverage on ordered Cu₃Au(001)

3.2 $[\text{Fe}(15\text{Å})/\text{Pd}(40\text{Å})]_{30}$ multilayer

The structure and magnetism of polycrystalline Fe/Pd multilayers have been investigated by Mühlbauer *et al.*,²⁰ and stabilization of high-moment fcc Fe in these multilayers with $\mu_{\text{Fe}} = 2.7 \pm 0.1 \mu_{\text{B}}$ has been reported. The lattice parameter perpendicular to the film plane in the fcc Fe layers was found to be 3.64 Å by X-ray diffraction.²⁰ Assuming the same in-plane lattice spacing in the Fe films and in the Pd layers, i.e. 3.89 Å (like bulk Pd), we can calculate $V_{\text{at}} = 12.06 \text{ Å}^3$ or $r_{\text{ws}} = 2.684 \text{ a.u.}$ for the Fe atomic volume or Wigner-Seitz radius, respectively, in the multilayer. These are larger values as compared to 4 ML Fe/Cu₃Au(001). The question of the in-plane lattice spacing in Fe layers on Pd is answered by RHEED experiments on epitaxial Fe single layers deposited on a Pd(001) buffer layer on Al₂O₃(11-20) (sapphire).³⁰ RHEED along the [011] azimuth of 15 and 40 Å thick Fe layers on Pd(001) layers exhibit 3D-type diffraction patterns (not shown) and an in-plane spacing with increasing Fe coverage that is indistinguishable from the Pd(001) in-plane spacing. However, the out-of-plane lattice spacing is found to decrease with increasing Fe coverage: for an uncovered epitaxial 15 Å thick Fe layer on Pd(001) a value of $c_0 = 3.2 \text{ Å}$ is obtained from the 3D-type RHEED pattern. By using the in-plane lattice parameter of Pd, i.e. 3.89 Å , and $c_0 = 3.2 \text{ Å}$ for the perpendicular lattice parameter, the Fe atomic volume is calculated to be $V_{\text{at}} = 12.11 \text{ Å}^3$, or $r_{\text{ws}} = 2.69 \text{ a.u.}$ These values are similarly high as for the case of the Fe/Pd multilayer described above.

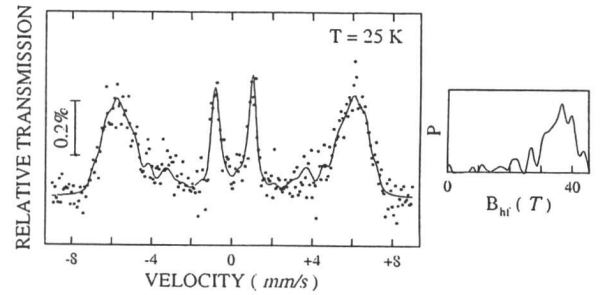


Fig. 6. Mössbauer (CEM) spectrum of 4 ML fct Fe on Cu₃Au(001) measured in-situ in UHV at 25 K. The experimental data were least-square fitted with a distribution of hyperfine fields, $P(B_{\text{hf}})$, shown on the right-hand side.

The magnetic properties of the $[\text{Fe}(15\text{Å})/\text{Pd}(40\text{Å})]_{30}$ multilayer has been determined by SQUID magnetometry and CEMS on the same sample. Fig. 7 shows the temperature dependence of the magnetization (normalized to the total mass of the Fe layers in the Fe/Pd multilayer). At low T the magnetization approaches a saturation value of $277 \text{ emu/g}_{\text{Fe}}$ (emu per g of Fe). This value is enhanced by 24.8 % with respect to the saturation magnetization of bulk bcc Fe ($221.9 \text{ emu/g}_{\text{Fe}}$ ³¹). Mühlbauer *et al.* have demonstrated that this strong magnetization enhancement is not caused by ferromagnetic polarization of Pd interface layers by the neighboring Fe layers.²⁰

Therefore, the enhancement is a property of the tetragonally distorted (fct) Fe structure in Fe/Pd multilayers.

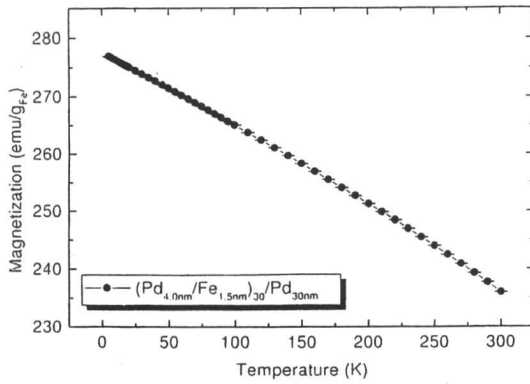


Fig. 7. Magnetization versus temperature of $[\text{Fe}(15\text{\AA})/\text{Pd}(40\text{\AA})]_{30}$ multilayer on sapphire

The CEM spectrum of the $[\text{Fe}(15\text{\AA})/\text{Pd}(40\text{\AA})]_{30}$ multilayer at 300 K and ~ 5 K is shown in Fig. 8. The spectra are characterized by a well-resolved magnetic Zeeman splitting with broadened lines due to a distribution of hf fields, $P(B_{\text{hf}})$. The spectra were least-squares fitted with two spectral contributions: (I) a sextet with rather sharp (Gaussian) lines and a large relative area of 67.3% (at 300 K) or 60.0 % (at 5 K), which we attribute to the interior of the Fe layers; (II) a less intense sextet of 32.7 % (at 300 K) or 40.0 % (at 5 K) relative spectral area with asymmetric lines due to a $P(B_{\text{hf}})$ distribution (Fig. 8, right-hand side), which we assign to Fe atoms located in the Fe/Pd interface region. This means that a thickness of about 2.5 - 3.0 Å Fe at every interface is affected by Pd atoms. The isomer shift δ at 300 K (relative to bulk bcc Fe at 300 K) was measured to be $+0.036 \pm 0.008$ mm/s for subspectrum (I), and $+0.129$ mm/s (average value) for subspectrum (II) (interface). A small positive isomer shift, such as for the film interior ($+0.036$ mm/s), has been observed also for FM fct-Fe on Cu(001),⁵⁾ and thus gives support to the conclusion on the structure from X-ray diffraction²⁰⁾ and RHEED results in the Fe/Pd system.

The hf field of the fct-Fe film interior is 33.3 ± 0.1 T at 300 K (accidentally similar to that of bulk bcc Fe at 300 K: 33.3 T), and 37.8 ± 0.4 T at ~ 5 K. The latter value is enhanced by 11.2 % with respect to that of bulk bcc Fe (34.0 T at ~ 5 K). However, this enhancement of the hf field is only about half of the magnetization enhancement (24.8%) in the same sample. Nevertheless, these results prove that fct-Fe in Fe/Pd multilayers is in a high-moment state.

The spontaneous Fe spin direction in the multilayer was found to be preferentially oriented in the film plane at 300 and ~ 5 K. This result follows from the line intensity ratios in the Mössbauer spectra. For the interface fraction we obtain hf fields with average values of 29 ± 0.5 T at 300 K and 32.3 ± 0.6 T at ~ 5 K; these values are reduced with respect to the corresponding values in the film interior.

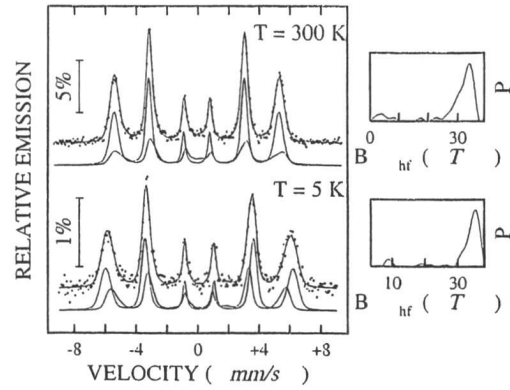


Fig. 8. Mössbauer (CEM) spectrum of $[\text{Fe}(15\text{\AA})/\text{Pd}(40\text{\AA})]_{30}$ multilayer on sapphire, measured ex-situ at 300 K (top) and ~ 5 K (bottom). Right-hand side: distribution of hyperfine fields, $P(B_{\text{hf}})$.

§4. Conclusion

The experimental results are summarized in Fig. 9 which exhibits the correlation of the hf field, B_{hf} , measured at low T (near magnetic saturation) and the measured Wigner-Seitz radius, r_{ws} , for fcc-like Fe systems including the cases of the Fe/Cu₃Au(001) film and the Fe/Pd multilayer investigated in the present work. Comparison with Fig. 1 shows that a plot of B_{hf} ver-

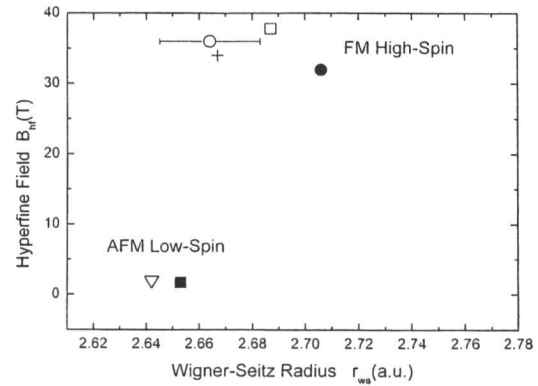


Fig. 9. Hyperfine field near magnetic saturation as a function of the measured Wigner-Seitz radius, r_{ws} , for fcc-like Fe systems. Open triangle: AFM fcc Fe precipitates in Cu matrix at 4.2 K.⁴⁾ Full square: 300-K grown AFM 5-10 ML fcc-Fe/Cu(001) at 35 K.⁴⁾ Full circle: 300-K grown FM fct-Fe/Cu(001) at 40-55 K.⁴⁾ Open circle: 313-K grown FM 4.0 ML fct-Fe/Cu₃Au(001) at 25 K (present work). Open square: 300-K grown FM $[\text{fct-Fe}(15\text{\AA})/\text{Pd}(40\text{\AA})]_{30}$ multilayer at ~ 5 K (present work). The data point for bulk bcc Fe (cross) at 4.2 K is shown for comparison. (The temperatures stated are the measurement temperature for the hyperfine field. For full square and full circle: r_{ws} was calculated by using the out-of-plane lattice parameter from LEED^{10,16)} and the in-plane lattice spacing from RHEED¹⁴⁾).

sus the nominal r_{ws} values of the substrate is by no means justified for Fe films, because in reality the films are tetragonally distorted in a way that depends on the specific substrate used (Cu, Cu₃Au or Pd), and also the in-plane atomic distance may differ from that of the sub-

strate¹⁴⁾ The highest rws value is achieved in FM expanded fcc (fct-) Fe films on Cu(001), followed (in descending order) by compressed fcc (fct-) Fe films in our Fe/Pd multilayer and the compressed fcc (fct-) Fe film (4ML) on Cu₃Au(001). This group of data points exhibits hyperfine fields between 32-38 T, indicating the high-spin state. It is interesting that the data points for Fe/Cu₃Au(001) and for the Fe/Pd multilayer are close to the value for bulk bcc Fe (cross in Fig. 9). However, the shape and spectral parameters of our Mössbauer spectra prove, that the present Fe/Cu₃Au(001) and [Fe/Pd]₃₀ films (and also earlier Fe/Cu(001) films⁵⁾) definitely do not have properties like bulk bcc Fe. These spectra are rather typical for distorted fcc (fct) high-spin Fe films.

The data points for AFM low-spin Fe in Fig. 9 are located at lower rws values than those of FM high-spin Fe. Fig. 9 shows that the AFM low-spin to FM high-spin transition in fcc-like Fe occurs very abruptly near $r_{ws} \simeq 2.66$ a.u.

Acknowledgment

We are indebted to Ulrich von Hörsten for his most valuable technical assistance. Work supported by Deutsche Forschungsgemeinschaft (SFB 491).

- 1) V.I. Moruzzi, P.M. Marcus, and J. Kübler, *Phys. Rev.* **B39** (1989) 6957, and references cited therein.
- 2) G.L. Krasko and G.B. Olson, *Phys. Rev.* **B40** (1989) 11536
- 3) C.H. Herper, E. Hoffmann, and P. Entel, *Phys. Rev.* **B60** (1999) 3839, and references cited therein
- 4) T. Shinjo and W. Keune, *J. Magn. Magn. Mater.* **200** (1999) 598, and references therein.
- 5) W. Keune, A. Schatz, R.D. Ellerbrock, A. Fuest, Katrin Wilmers, and R.A. Brand, *J. Appl. Phys.* **79** (1996) 4265, and references cited therein
- 6) Y. Yamada, B. Sadeh, C.Lee, M. Doi, and M. Matsui, *J. Magn. Soc. Japan* **23** (1999) 575
- 7) A. Clarke, P.J. Rous, M. Arnott, G. Jennings, and R.F. Willis, *Surf. Sci.* **192** (1987) L843
- 8) P. Ehrhard, B. Schönfeld, H.H. Ettwig, and W. Pepperhoff, *J. Magn. Magn. Mater.* **22** (1980) 79
- 9) D. Schmitz, C. Charton, A. Scholl, C. Carbone, and W. Eberhardt, *Phys. Rev.* **B59** (1999) 4327
- 10) S. Müller, P. Bayer, C. Reischl, K. Heinz, B. Feldmann, H. Zillgen, and M. Wuttig, *Phys. Rev. Lett.* **74** (1995) 765
- 11) J. Thomassen, F. May, B. Feldmann, M. Wuttig, and H. Ibach, *Phys. Rev. Lett.* **69** (1992) 3831
- 12) D. Li, M. Freitag, J. Pearson, T.Q. Qiu, and S.D. Bader, *Phys. Rev. Lett.* **72** (1994) 3112
- 13) S. Müller, A. Kinne, M. Kottcke, R. Metzler, P. Bayer, L. Hammer, and K. Heinz, *Phys. Rev. Lett.* **75** (1995) 2859
- 14) A. Schatz and W. Keune, *Surf. Sci.* **440** (1999) L841
- 15) r_{ws} is given by $4\pi r_{ws}^3/3 = a^3/4$ for the fcc lattice, a = lattice parameter. The atomic unit (a.u.) is the first Bohr radius, $a_0 = 5.292 \times 10^{-11}$ m.
- 16) P. Bayer, S. Müller, P. Schmailzl, and K. Heinz, *Phys. Rev.* **B48** (1993) 17611
- 17) T. Ezawa, W.A.A. Macedo, U. Glos, W. Keune, K.P. Schletzt, and U. Kirschbaum, *Physica B* **161** (1989) 281
- 18) W. Keune, T. Ezawa, W.A.A. Macedo, U. Glos, K.P. Schletzt, and U. Kirschbaum, *Physica B* **161** (1989) 269
- 19) D.J. Keavney, D.F. Storm, J.W. Freeland, I.L. Grigorov, and J.C. Walker, *Phys. Rev. Lett.* **74** (1995) 4531
- 20) H. Mühlbauer, Ch. Müller, and G. Dumpich, *J. Magn. Magn. Mater.* **192**(1999) 423
- 21) Ch. Müller, H. Mühlbauer, and G. Dumpich, *Thin Solid Films* **310** (1997) 81
- 22) J. Henry, V. Pierron-Bohnes, P. Vennégues, and K. Ounadjela, *J. Appl. Phys.* **76** (1994) 2817
- 23) M.A. Van Hove, W.H. Weinberg, and C.-M. Chan, *Low-Energy Electron Diffraction* (Springer, Berlin 1986) p. 105
- 24) R. Rochow, C. Carbone, Th. Dodt, F.P. Johnen, and E. Kisker, *Phys. Rev.* **B41** (1990) 3426
- 25) A.A. Hezaveh, G. Jennings, D. Pescia, R.F. Willis, K. Prince, M. Surman, and A. Bradshaw, *Solid State Commun.* **57** (1986) 329
- 26) F. Baudelet, M.-T. Lin, W. Kuch, K. Meinel, B. Choi, C.M. Schneider, and J. Kirschner, *Phys. Rev.* **B51** (1995) 12563
- 27) M.-T. Lin, J. Shen, W. Kuch, H. Jenniches, M. Klaua, C.M. Schneider, and J. Kirschner, *Phys. Rev.* **B55** (1997) 5886
- 28) B. Feldmann, B. Schirmer, A. Sokoll, and M. Wuttig, *Phys. Rev.* **B57** (1998) 1014
- 29) B. Schirmer, B. Feldmann, and M. Wuttig, *Phys. Rev.* **B58** (1998) 4984
- 30) T. Steffl, unpublished
- 31) D.H. Martin, *Magnetism in Solids* (The M.I.T. Press, Cambridge, Massachusetts, USA, 1967) p. 10